

Article

Influence of Environmental Factors on the Sap Flow Activity of the Golden Pear in the Growth Period of Karst Area in Southern China

Bo Fan ^{1,2}, Ziqi Liu ^{1,2}, Kangning Xiong ^{1,2,*}, Yuan Li ^{1,2} , Kaiping Li ^{1,2} and Xiao Yu ^{1,2}

¹ School of Karst Science, Guizhou Normal University, Guiyang 550001, China; 17793689707@163.com (B.F.); 201511004@gznu.edu.cn (Z.L.); liyuan7pro@163.com (Y.L.); likaiping3extra@163.com (K.L.); yuxiao20200219@163.com (X.Y.)

² State Engineering Technology Institute for Karst Desertification Control, Guiyang 550001, China

* Correspondence: xiongkn@163.com

Abstract: Under extreme drought and climate change, golden pear trees have experienced problems such as yield reduction, dryness and death. This suggests that we know very little about the mechanisms regulating pear tree growth, assuming that meteorological factors positively influence plant sap flow. Based on this, we used the heat ratio method to monitor the sap flow of pear trees from June to December 2020, and recorded the changes in various environmental factors. The results showed that: (1) Sap flow velocity has obvious radial variability in tree sections; the sap flow velocity during the day was significantly higher than that at night ($p < 0.05$) and was higher in the growing season than in the non-growing season. (2) All environmental factors, except relative humidity and precipitation, were positively correlated with sap flow, vapor pressure deficit and photosynthetically active radiation, which are the key factors affecting daytime flow, and vapor pressure deficit and plant water potential are the key factors affecting nighttime flow. The linear regression results also showed that the daytime sap flow had a significant positive effect on the nighttime sap flow ($p < 0.05$). (3) The contribution of night flow to total daily flow varied from 17.3% to 50.7%, and most of the non-growing season values were above 40%. The results show that nighttime sap flow accounts for a significant portion of the pear tree's water budget. Continuous irrigation during fruit enlargement and non-growing seasons will increase fruit yield and maintain plant sap flow activity to avoid death due to drought.

Keywords: sap flow; drought stress; environmental factors; principal component analysis



Citation: Fan, B.; Liu, Z.; Xiong, K.; Li, Y.; Li, K.; Yu, X. Influence of Environmental Factors on the Sap Flow Activity of the Golden Pear in the Growth Period of Karst Area in Southern China. *Water* **2022**, *14*, 1707. <https://doi.org/10.3390/w14111707>

Academic Editor: Guido D'Urso

Received: 8 April 2022

Accepted: 24 May 2022

Published: 26 May 2022

Publisher's Note: MDPI stays neutral with regard to jurisdictional claims in published maps and institutional affiliations.



Copyright: © 2022 by the authors. Licensee MDPI, Basel, Switzerland. This article is an open access article distributed under the terms and conditions of the Creative Commons Attribution (CC BY) license (<https://creativecommons.org/licenses/by/4.0/>).

1. Introduction

Extreme drought conditions will seriously affect the survival and growth of vegetation and may jeopardize the sustainability of agriculture, forestry and other surface systems [1]. The main path of plant water loss, transpiration, is also an important part of the water budget of forest ecosystems, and is affected by both environmental factors and species characteristics [2]. The monitoring of tree trunk sap flow provides the water use status of plants throughout the year and also shows the characteristics of plant transpiration under different meteorological conditions and soil moisture environments. This helps us understand the response of plants to the external environment and avoid the death of plants due to climate change. The water support of transpiration mainly comes from soil water sources, and sufficient soil water can accelerate stand transpiration; the two are positively correlated on an interannual time scale [3–8]. The physiological responses of trees to soil moisture changes and drought varied significantly among different species.

In sap flow measurement based on instantaneous data, daily sum, or average, it can be found that on a daily scale, tree sap flow has a very significant relationship with meteorological factors, especially PAR (photosynthetically active radiation) and VPD (saturated

water pressure difference) [2,4]. In addition, it is also closely related to physiological factors such as canopy width and leaf area index, and environmental factors such as solar radiation, RH (relative humidity), T_a (air temperature), and VWC (soil water content) [9]. In most studies, sap flow rates decreased when vapor pressure deficit, air temperature, and soil moisture decreased, while relative humidity changed in the opposite direction. Environmental factors such as a strong evaporation effect and high temperature become driving factors of tree sap flow activities in arid areas [10]. In addition, wind can damage the tree canopy and dry out the available moisture on the leaves, and air temperature may also have a significant effect on stomata conductance, which will lead to changes in sap flow rates. However, the interaction between different environmental factors is complex, and there is often a high correlation between many meteorological variables that affect sap flow rates [11,12]. However, previous studies have found that even during the non-growing season, when leaves are falling, there is still weak fluid flow activity. In evergreen plants, night-time transpiration occurs because their stomata are not completely closed at night; the transpiration of deciduous plants in the leafless state is more likely due to water redistribution driven by water potential differences in plants, especially in arid environments [11].

Studies have shown that plants' water relationships change in arid environments; under the response of stomata to external factors, sap flow can decrease, remain constant, or increase [13]. Stomata closure due to severe plant water loss or leaf loss due to severe drought will result in decreased fluid flow. Plant leaf shedding maintains the hydraulic conductivity of the whole plant, reducing the water use of plants at specific vapor pressure deficits; however, increased evaporation may also drive water use of the whole plant [14,15]. A significant relationship has also been found between tree stem water storage and tree size. The water storage of larger trees could alleviate the damage caused by soil drying, and the sap flow value of larger trees was always to be higher than that of smaller trees, so soil water content had a greater impact on smaller trees, which may be related to the root depth of trees [16]. The theory of hydraulic niche separation suggests that different plant species can coexist continuously because they can adopt different hydraulic strategies in complex environments; deep-rooted plants can obtain underground water to maintain their hydraulic balance, while shallow-rooted plants rely on rain and are greatly affected by external influences [17,18]. In addition, xylem characteristics also affect plant hydraulic transport, such as catheter size, intact branching density, and fiber size [19]. Trees in arid regions have narrow xylem ducts and dense intact branches, which will increase resistance to water flow during precipitation and reduce transpiration rates and plant growth; however, narrow ducts also reduce xylem resistance to cavitation, resulting in high plant mortality.

Large-scale estimates of regional vegetation growth rely on remote sensing techniques, while the sap flow monitoring of specific trees mainly relies on the heat ratio method (HRM), heat field deformation (HFD), thermal dissipation probe (TDP) and other means. The HRM was developed by scientists at the University of Western Australia in the late 1990s in response to the limitations of existing sap flow measurement techniques. This technique is a modification of the Compensated Thermal Pulse Method (CHPM) that allows the measurement of very slow flow rates and even reverse sap flow to improve CHPM, allowing the monitoring of water flow in stems and roots of a wide variety of species, sizes and environmental conditions. It can detect and quantify low flow more reliably than other techniques [20,21]. Zhao et al. have relied on this technology to study the trend in liquid flow of *Populus euphratica* in the Heihe River Basin of China [11].

The golden pear (Latin name: *Pyrus pyrifolia* Nakai, hereinafter referred to as golden pear) is a new variety of pear bred in the 20th century. It has the reputation of "fruit family" and "natural mineral water". It usually blooms in late February to early March and mid-March to early April. Leaf buds sprout in early April and begin to sprout in mid-April. They bear fruit and ripen from late August to mid-September. At this time, in order to ensure high and stable yields, the requirement for irrigation is relatively high as

the trees require a huge amount of water. The fruit growth period is about 135 days and leaves fall in mid-November [22]. In the economically barren and backward karst areas, golden pears are an important industry to support local economic development. They have broad market prospects and are sought after by surrounding provinces and cities. While bringing huge economic value, they are also important to the karst area. Ecological restoration and soil and water conservation are of great significance [23,24]. There have been cases of weak, dry, and dead trees, and reduced fruit yields, and therefore finding a solution is urgent. Studying the changes between the sap flow of the golden pear tree trunk and external environmental factors to understand the water balance in the plant for precise irrigation is very important. The main purpose of this study is understanding the response of golden pear sap flow to external environmental factors, discuss the sap flow variation characteristics of golden pears during observation periods, determine the relationship and influencing factors of sap flow between the day and night, and determine the ratio of the night sap flow to total sap flow of golden pears. These questions will help us to strengthen our understanding of the growth characteristics of golden pears and guide villagers to carry out more precise irrigation work in the context of future climate change.

2. Materials and Methods

2.1. Study Sites

This study was conducted at the golden pear plantation base (27°09′45″ N, 108°09′28″ E) in Xiaowangjiazhuang Village, Baiduo Town, Shibing County, Guizhou Province, China (Figure 1). The area is located in the transition zone from Yunnan-Guizhou Plateau to the hilly plain in the east. The whole terrain slopes from south to north, with an average elevation of 1100 m. It belongs to the typical subtropical monsoon humid climate, with four distinct seasons and abundant sunshine, the climate is warm and humid. The annual average temperature in this region is 15 °C, and the annual average precipitation is 980–1180 mm. The sample site is located in a golden pear garden base built in 2016, covering an area of about 4000 hm², the average stand age is 4 years old, and the plants grow well and healthily. In the early stage of the experiment, we measured the physical and chemical properties of the soil in the sample site with the ring knife method. Soil bulk density was 1.29 g·cm⁻³, saturated water content was 45.7%, and soil capillary water holding capacity was 33.20%.

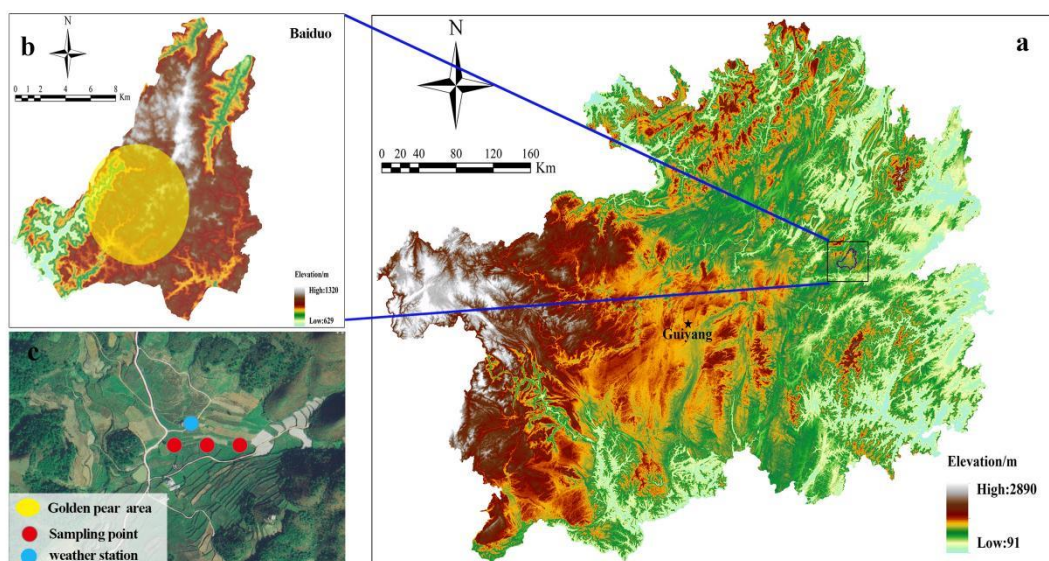


Figure 1. Location of the study area in Guizhou Province (a). The yellow area in the upper left corner represents the golden pear growth area (b), the red point in the lower left corner represents the sampling point, and the blue point represents the weather station (c).

2.2. Material

We selected three pear tree samples with basically the same DBH (diameter at breast height) in each of the three 10 m × 10 m sample areas; we determined that these sample trees were healthy and free of disease and insect pests during the experiment. These sample trees all have the same elevation, slope, and aspect, and the microgeomorphic environment is basically the same. We measured DBH at 1.3 m and estimated tree height and crown width using a DBH scale. DBH was 6.9 ± 0.62 cm, average height was 1.98 ± 0.15 , and average crown width was 2.1 ± 1.4 (Table 1).

Table 1. Summary of biological parameters of sample trees in the study area.

Sample Area	DBH (cm)	Height (m)	Crown Width	Age of Stand
1	6.2	1.84	2.0 m × 1.38 m	4
2	7.1	1.96	2.1 m × 1.40 m	4
3	7.4	2.15	2.2 m × 1.43 m	4
Mean ± SD	6.9 ± 0.62	1.98 ± 0.15	2.1 ± 1.40	4 ± 0

2.3. Sap Flow and Water Potential Measurement

From 1 June 2020 to 31 December 2020, we measured sap from selected trees using the heat ratio flow technique. A sap flow sensor and plant stem infiltration water potential meter were installed at 1.3 m from the ground of the selected sample tree (Figure S1). We used HRM sap flow sensors (SFM1, ICT International Pty Ltd., Armidale, Australia, measuring range: -100 to $+100$ cm h^{-1} , measuring accuracy: 0.5 cm \cdot h^{-1}), which consist of a heater and two temperature probes (35 mm) located above and below the heater. We drilled three parallel 35 mm deep holes perpendicular to the stem using an instrument-specific drill bit and inserted the probes in sequence. In order to avoid differences in environmental factors, all sensors were located in the north; to prevent mosquito damage and extreme weather interference, the surface was covered with tinfoil to ensure continuous and accurate monitoring of the instrument.

The heating needle provides 20 J heat pulses of 2.5 s every 10 min. Each temperature probe has two thermistors that can be measured independently from 7.5 mm and 22.5 mm away from the top. All sap flow sensors are powered by an external 12 v deep cycle Marine battery, which is recharged via solar panels. The thermal pulse velocity was measured every 10 min, and the data were recorded in the SD card inside the instrument. A plant stem osmotic water potential meter (PSY1, ICT International Pty Ltd., Australia, measuring range: -0.1 – 10 Mpa, measuring accuracy: ± 0.1 Mpa) was used to monitor plant water potential in conjunction with sap flow.

The sap flow was calculated by the temperature difference between the upper and lower probes, and according to Granier's empirical formula (1987) [25]:

$$k = \frac{\Delta T_{\max} - \Delta T}{\Delta T} \quad (1)$$

where k represents the infinite compendium constant, related to the temperature difference between the two probes, ΔT_{\max} is the maximum value between the upper and lower probes when the flow is equal to zero, and ΔT is the difference between the temperature measured by the upper and lower probes ($^{\circ}\text{C}$).

$$Vs = 0.0119 \times K^{1.231} \times 3600 \quad (2)$$

$$F = Vs \times As \quad (3)$$

where Vs is the sap velocity ($\text{cm} \cdot \text{h}^{-1}$), As is the sapwood area (cm^2), and F is sap flow rate ($\text{cm}^3 \cdot \text{h}^{-1}$).

2.4. Soil Water Potential and Soil Water Content Measurement

We dug a 40 cm deep soil profile 50 cm away from the root of the selected tree and installed a soil moisture sensor (ECH₂O-5TE, METER Group Inc., Pullman, WA, USA, Soil moisture: measurement range 0–100%; measurement accuracy $\pm 3\%$) and an MPS-6 soil moisture potential sensor (Pullman, WA, USA, resolution 0.1 kPa 0.1 °C; range –9 kPa–100 kPa) at 0–15 cm and 15–30 cm, respectively. There were four layers of sensors in each section, recording soil water potential, temperature, conductivity, and water content in real time. Data were observed every 30 min and logged to the Em50 (Z6-05376, Pullman, WA, USA) data collector.

2.5. Measurement of Environmental Factors and Calculation

Environmental factors were measured in real time by a small weather station (Pullman, WA, USA) 20 m away from the plot. Measurement elements include RH, Ta, P and PAR. The weather station recorded the value every 30 min. VPD was calculated from air temperature and relative humidity according to Campbell and Norman (1998) [26], as follows:

$$VPD = 0.611 \times e^{\left(\frac{17.502 \times T_a}{T_a + 240.97}\right)} \times (1 - RH) \quad (4)$$

where VPD is the saturated water vapor pressure difference, Ta is the temperature, RH is the relative humidity, and e is the exponential function.

2.6. Data Analysis

We defined 6:00 to 18:00 as “day” and the rest as night. The whole pear tree growing season is from June to September, and the fruit is picked by the end of September. Considering the entire pear tree growth cycle, we defined May to September as the growing season and October to December as the non-growing season. The non-growing season begins with a new round of pruning. All data except precipitation were summarized at hourly intervals and expressed as mean and standard error. The sap flow tool (ICT International Pty Ltd., Armidale, NSW, 2350, Australia, Version 1.5, <http://www.sapflowtool.com/SapFlowToolContact.html>, accessed on 17 September 2020) was used to analyze the monitored data to obtain sap velocity ($\text{cm} \cdot \text{h}^{-1}$) and sap flow rate ($\text{cm}^3 \cdot \text{h}^{-1}$). The sap flow out value measured by the instrument was used for subsequent analysis. Changes in daily flow were compared using line graphs.

Bivariate correlation analysis was used to detect the correlation between environmental factors ($p < 0.05$). One-way ANOVA with a significance level $\alpha = 0.05$ was used to test the difference between the day and night mean values of sap flow in each month, combined with Tukey’s posttest, multiple comparisons were performed on the continuous measurement data. Volumetric water content, plant water potential, soil water potential, and sap flow were tested by the Tukey-Kramer multiple mean comparison. Principal Component Analysis (PCA) was used to determine the leading factors of each environmental factor. By fitting the linear function, the response degree of sap flow of pear tree to environmental variables was determined, as well as the relationship between daytime sap flow and nighttime sap flow. All analyses were performed using SPSS 23 (Version 23, IBM, Foster City, CA, USA) and Origin 2021 (OriginPro2021, V9.8, OriginLab, Northampton, MA, USA) mapping.

3. Results

3.1. Monthly Variation in Meteorological Factors and Soil Moisture Content during the Study Period

The environmental factors showed significant seasonal variations throughout the study period; they gradually increased from May, reached the maximum value in July and August, and declined from September until the end of December (Figure 2). During the whole monitoring period, the average daily temperature reached 16.44 °C, 22.29 °C in the growing season, and 8.69 °C in the non-growing season. Fluctuations in temperature and RH led to significant changes in VPD (0.051–1.151 MPa), the peak of PAR occurred

on 6 June, when the sun's rays were intense; the maximum monthly mean value was $352.1 \mu\text{mol m}^{-2}\cdot\text{s}^{-1}$ in August (Table 2). The changes of VPD and PAR were basically the same, and they entered a stable state from September.

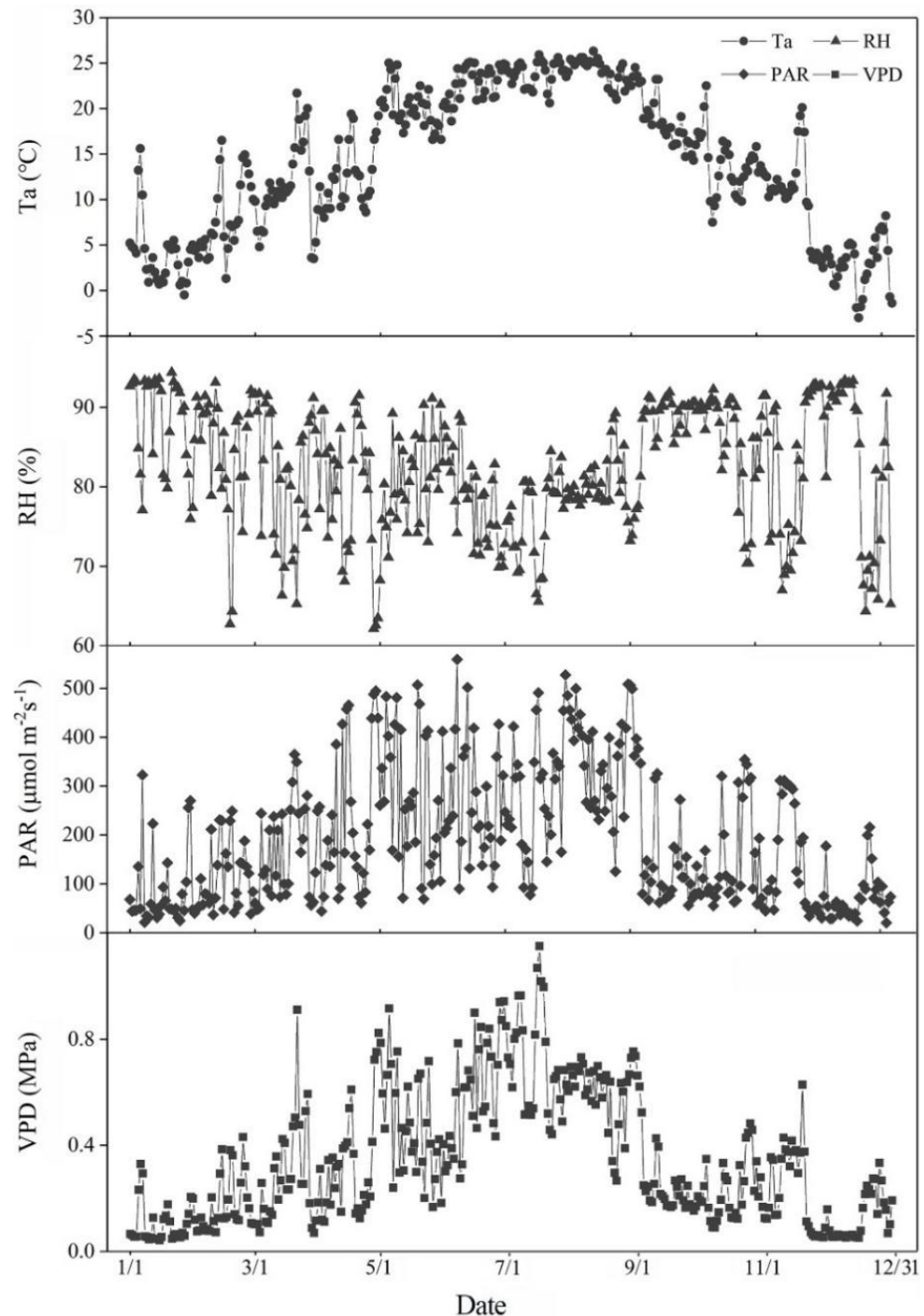


Figure 2. Monthly trends of environmental factors affecting tree sap flow activity during the 2020 study period. From top to bottom are temperature (Ta), relative humidity (RH), photosynthetically active radiation (PAR), and saturated water pressure difference (VPD). As an environmental factor affecting tree growth, it has an inseparable impact on plant sap flow activity and therefore requires monitoring.

Table 2. Descriptive statistics for four environmental factors. From top to bottom are 1 to 12 months, the data structure is mean + standard error, all values are kept to two decimal places.

Mouth	RH (%)	Ta (°C)	PAR ($\mu\text{mol m}^{-2}\cdot\text{s}^{-1}$)	VPD (MPa)
January	88.30 ± 5.90	3.90 ± 3.50	83.90 ± 77.20	0.10 ± 0.10
February	84.70 ± 7.50	8.00 ± 4.10	113.60 ± 93.80	0.20 ± 0.10
March	81.70 ± 8.00	11.30 ± 4.60	166.30 ± 93.80	0.30 ± 0.20
April	78.84 ± 8.68	12.80 ± 8.68	230.56 ± 145.42	0.34 ± 0.21
May	81.25 ± 5.39	20.20 ± 2.23	275.20 ± 135.02	0.46 ± 0.19
June	78.02 ± 5.34	23.00 ± 1.79	268.20 ± 116.19	0.63 ± 0.20
July	76.37 ± 5.15	23.90 ± 1.76	299.30 ± 127.53	0.71 ± 0.19
August	80.06 ± 3.72	24.00 ± 1.76	352.10 ± 95.74	0.60 ± 0.13
September	88.73 ± 3.07	18.10 ± 2.42	141.20 ± 89.95	0.24 ± 0.11
October	85.42 ± 6.51	13.50 ± 3.07	148.90 ± 99.20	0.23 ± 0.11
November	82.78 ± 8.97	9.80 ± 4.81	143.00 ± 103.20	0.23 ± 0.15
December	82.97 ± 10.55	2.80 ± 2.82	69.00 ± 45.80	0.13 ± 0.09

The rainfall distribution during the study period was extremely uneven (Figure 3), 90.4% of rainfall occurred from June to September; compared with 2019, the rainfall and temperature in 2020 showed more and higher trends (Figure S2). Influenced by seasonal rainfall, VWC also showed high monthly differences. From June to mid-July, soil water content has always maintained a stable trend. After a significant precipitation event on July 20, soil water content increased slightly for the next two or three days, but continued to decline thereafter. The water content also showed a trend of first increasing and then decreasing under several precipitation events in August and September. Although the precipitation in August and September was significantly higher than in October, soil water content was significantly lower than in October. This may be related to the fact that pear trees are in the fruit expansion stage, and the demand for water in the fruit ripening stage is relatively high, which consumes a lot of water, resulting in soil water depletion. In the growing season, affected by the water absorption of plants, the water content of the 0–15 cm soil profile is mostly lower than 15–30 cm.

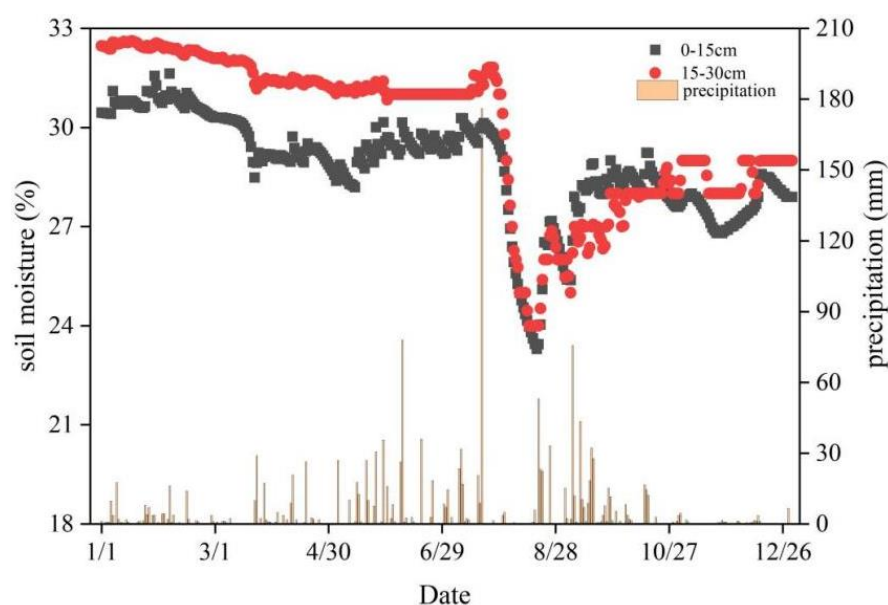


Figure 3. Changes in precipitation and soil moisture in the study area throughout the 2020 observation period. The black dots in the figure represent the soil water content of 0–15 cm, the red dots represent the soil water content of 15–30 cm, and the rectangles represent the precipitation. The water supply status of plants can be judged by the changes in precipitation and soil water content.

3.2. Changes in Radial Flow Velocity and Sap Flow

We imported the measured data into the sap flow tool for analysis and obtained the sap velocity and sap flow rate. A few typical sunny days in July and August of the growing season are shown as examples (Figure 4). From 30 July to 3 August, the daily flow rate showed the same trend. The sap flow velocity in the daytime was significantly higher than at night ($p < 0.05$). From 00:00 to 06:00, there was a steady change, with a minimum speed of $6.15 \text{ cm}\cdot\text{h}^{-1}$; the speed increased rapidly from 06:00 to 12:00, reached the maximum at 14:00 to 15:00, and then decreased throughout the evening, and slowly decreased from 21:00 to 00:00. The maximum value of the sap flow velocity at the outer 0.5–1 cm was $46.21 \text{ cm}\cdot\text{h}^{-1}$, and the minimum value of the sap flow velocity at the inner 2–2.5 cm was $36.03 \text{ cm}\cdot\text{h}^{-1}$ (Figure 4b). From the end of October, the external flow velocity ($5.14\text{--}6.62 \text{ cm}\cdot\text{h}^{-1}$) was always lower than the internal flow velocity ($6.95\text{--}8.15 \text{ cm}\cdot\text{h}^{-1}$). This is likely due to the Ta, PAR, and VPD weakening in autumn and winter; the lack of precipitation changed the pear tree water use strategy.

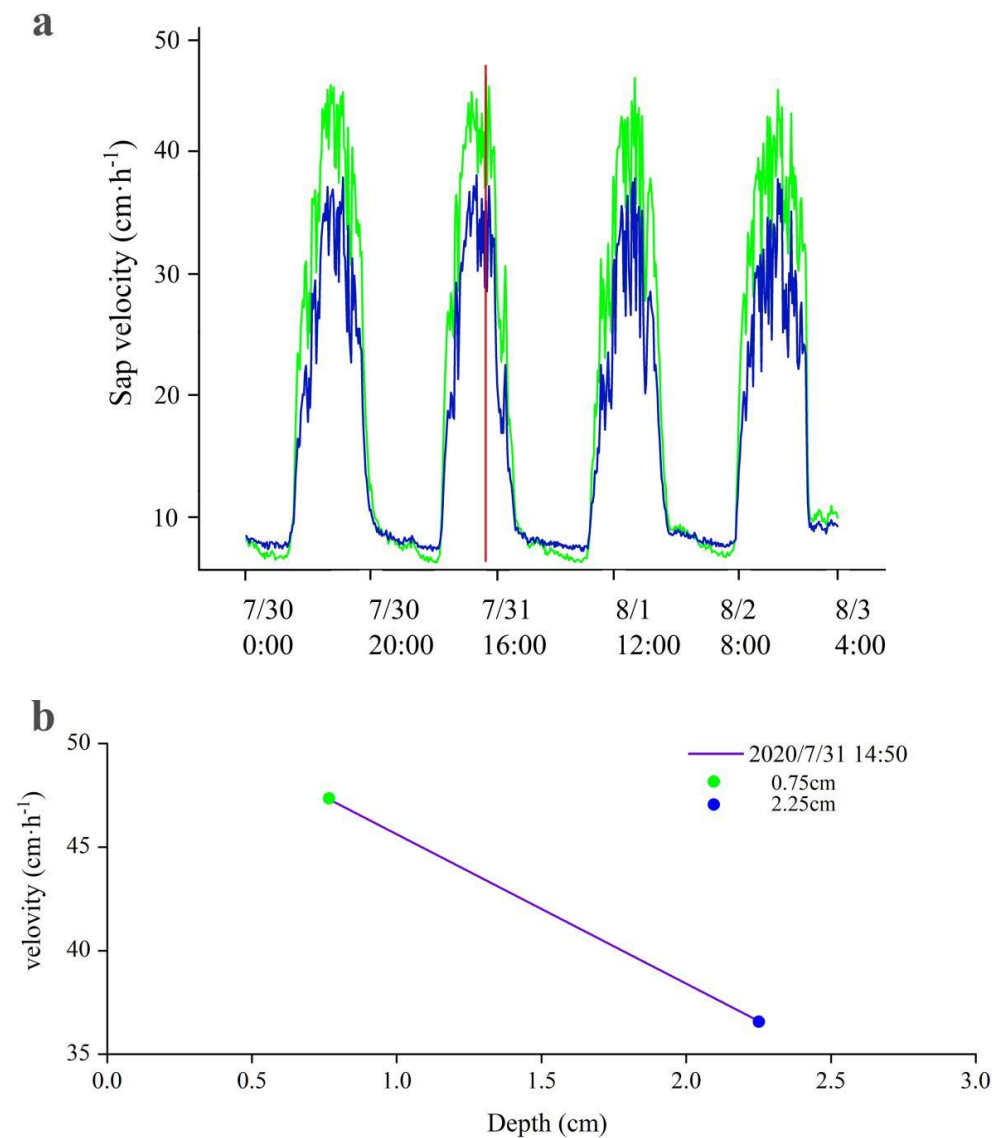


Figure 4. Changes in the sap flow of the Golden Pear from 30 July to 2 August 2020. (a) Flow rate variation. (b) Changes in the radial distribution of flow velocity at 14:50 on 31 July. The green line shows the sap flow rate at 0.75 cm from the tree, and the blue line shows the sap flow rate at 2.25 cm. The red line in (a) refers to the flow rate at 14:50 on 31 July, and the radial change is more clearly shown in (b). Graphics are drawn by origin software.

The probe's two thermistors showed a strong radial profile change in flow velocity, the flow velocity of the external (0.75 cm) was always lower than that of the internal (2.25 cm) during the day. The maximum internal and external flow velocities were $36.6 \text{ cm}\cdot\text{h}^{-1}$ and $47.43 \text{ cm}\cdot\text{h}^{-1}$, respectively. The flow velocity of the external flow was 1.29 times that of the internal flow (Figure 4b). At night, the internal flow velocity was usually slightly higher than the external flow velocity; they were $7.32 \text{ cm}\cdot\text{h}^{-1}$ and $6.19 \text{ cm}\cdot\text{h}^{-1}$, respectively, where the difference between the two was not obvious. The radial profile variation in sap flow velocity may be related to the tree itself; the deeper the xylem, the slower the sap flow velocity, while the surface layer is affected by the external environment.

3.3. Relationship between Sap Flow Change and Environmental Factors

As shown in Figure 5, the diurnal variation in sap flow is basically consistent with the diurnal variation in environmental factors but not necessarily synchronous. PAR reaches its maximum at 13:00, two hours earlier than T_a and VPD, whereas sap flow at 0:00–6:00 remained low, increased rapidly after sunrise, reached the daily peak at the same time or behind T_a , VPD and PAR, was lower at 18:00 and lowest at 23:00. At the same time, the diurnal variation in plant water potential was opposite to sap flow and environmental factors. It maintained a high water potential (-0.217 MPa) at night and after sunrise, with each environmental factor reaching the maximum value, the plant water potential gradually decreased and reached the lowest value (-0.465 MPa) at 13:00, indicating that the plant demand reached the maximum at this time. During the whole observation period, there was a significant difference between the sap flow of golden pears in the growing season and the non-growing season ($p < 0.05$); the highest sap flow rate in July was $0.269 \text{ kg}\cdot\text{h}^{-1}$; then, it was lower ($0.101 \text{ kg}\cdot\text{h}^{-1}$) in December. However, there was no significant difference in diurnal variation between seasons.

In order to characterize the relationship between various environmental factors, we used linear regression analysis to predict or estimate the dependent variable by the optimal combination of multiple independent variables, which is more effective than one independent variable and is in line with reality. It is also good at capturing linear relationships in datasets, and results are easy to interpret. Data correlation analysis showed that pear sap flow was significantly correlated with RH, T_a , PAR, VPD and VWC ($p < 0.05$) (Figure S3). The relationship between sap flow and VPD was strongest (determination coefficient was $R^2 = 0.870$), followed by PAR (determination coefficient was $R^2 = 0.802$). Similarly, the RMSE and MAE values of the two were also the smallest, indicating that the data has a small deviation. Linear regression was used to further estimate the relationship between sap flow rate and various environmental factors (Figure 6).

The results showed that all the environmental factors, except RH and P, had a significant influence on sap flow ($p < 0.05$). PAR and VPD had more influence on pear sap flow, with an R^2 of 0.6412 and 0.7554 ($p < 0.05$), respectively. The RH was basically inversely related to sap flow, it shows that the sap flow will decrease under the condition of high relative humidity. In the correlation analysis of environmental factors, there was a significant correlation between each factor quality (Figure S3); therefore, we used principal component analysis to extract the key factors. The results showed that the first two PCA axes explained 82.325% of the diurnal variation in the overall environment (Table 3); axis one explained 62.423% of the variation; it was significantly positively correlated with VPD ($p < 0.05$), and the factor load of VPD was 0.962. PAR showed a factor load of 0.898; axis two explained 18.902% of the difference and was significantly positively correlated with VWC ($p < 0.05$); the factor load of VWC was 0.948. The first two axes accounted for 81.328% of the nocturnal differences, and the first axis accounted for 57.268%. VPD also contributed the most, with a factor load of 0.962, which was slightly weaker than during the day. Axis two accounted for 24.060% of the nighttime variance, which was positively correlated with Ψ_{plant} ($p < 0.05$); the factor load was 0.871 (Figure 7a). In general, VPD, PAR, T_a , and VWC were the main factors affecting the daytime sap flow of pear trees, and at night, VPD and Ψ_{plant} were the main influences (Figure 7b).

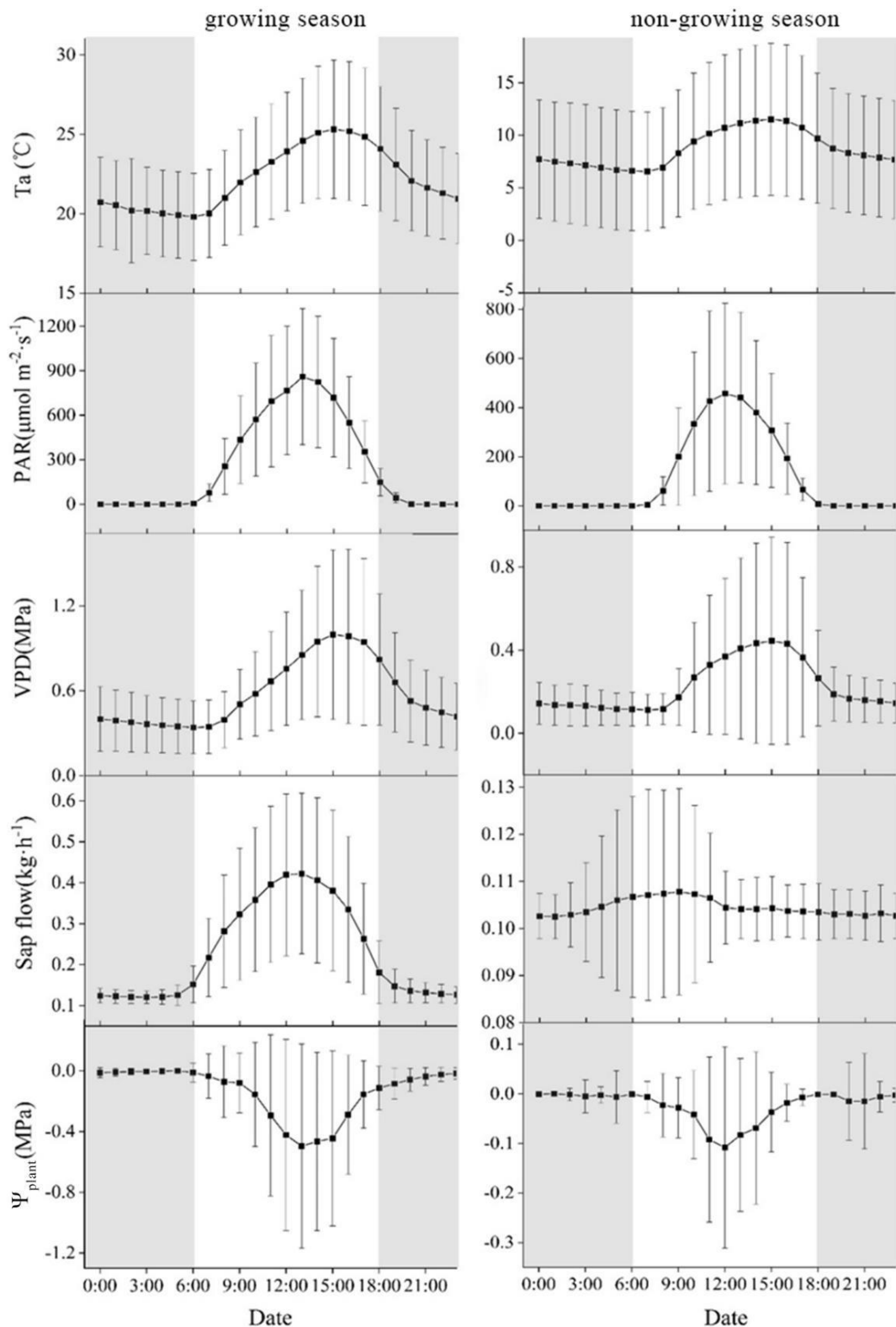


Figure 5. Diurnal variation in sap flow and environmental factors in growing and non-growing seasons during the whole study period. From top to bottom are temperature (T_a), photosynthetically active radiation (PAR), saturated water vapor pressure difference (VPD), sap flow and plant water potential (Ψ_{plant}). The left side of the figure represents the growing season, and the right side is the non-growing season. The gray shaded area in the figure represents night, and the white area represents day. All values are mean \pm SD. The significance level was $p < 0.05$.

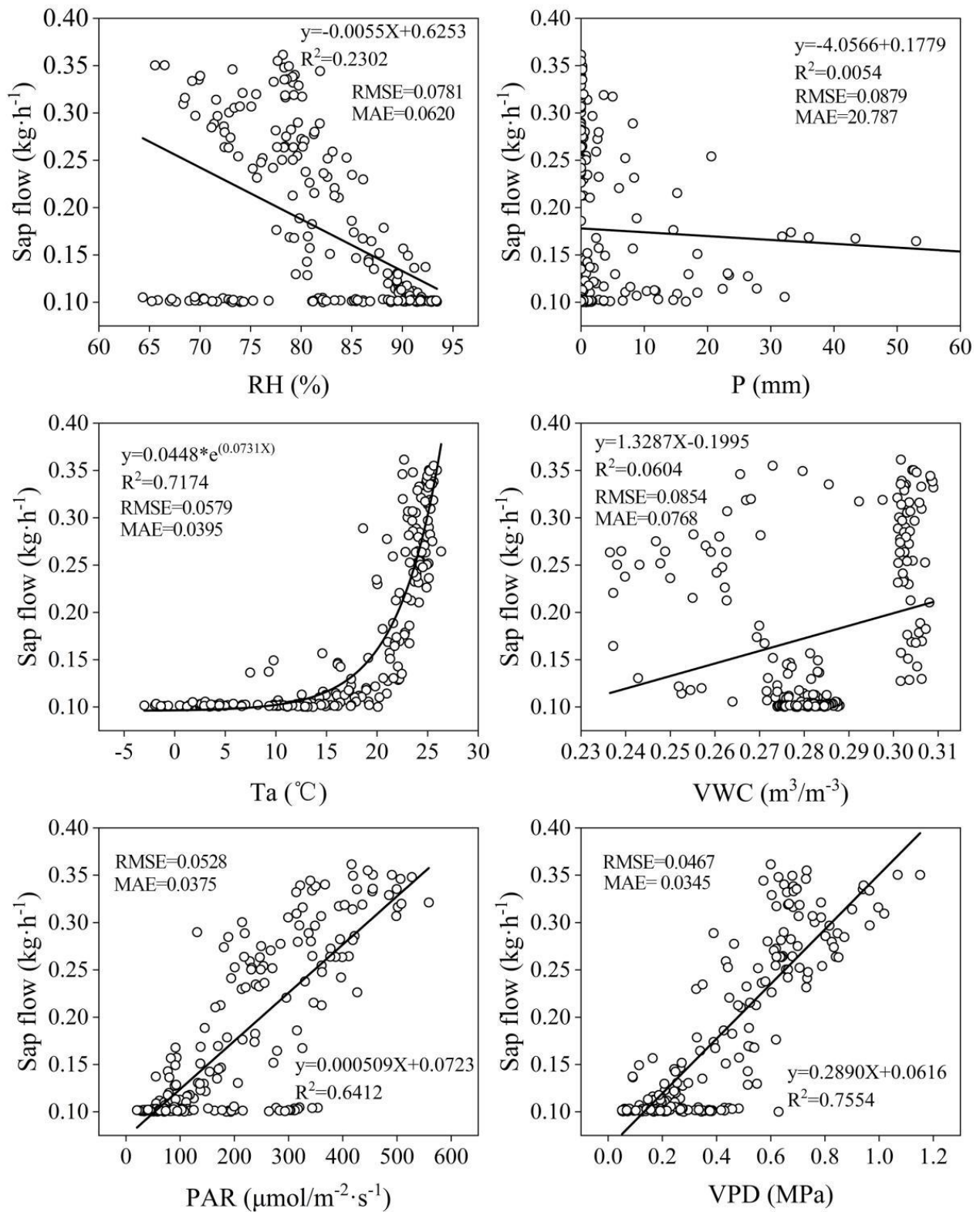


Figure 6. Linear regression analysis and nonlinear analysis of various environmental factors and liquid flow. The black circles in the figure represent each value, and the straight line represents the linearity. From top to bottom are RH: relative humidity; *p*: precipitation; Ta: air temperature; VWC: volumetric water content; PAR: photosynthetically active radiation; VPD: vapor pressure deficit. RMSE is root mean square error, MAE is mean absolute value error. Significance level $p < 0.05$.

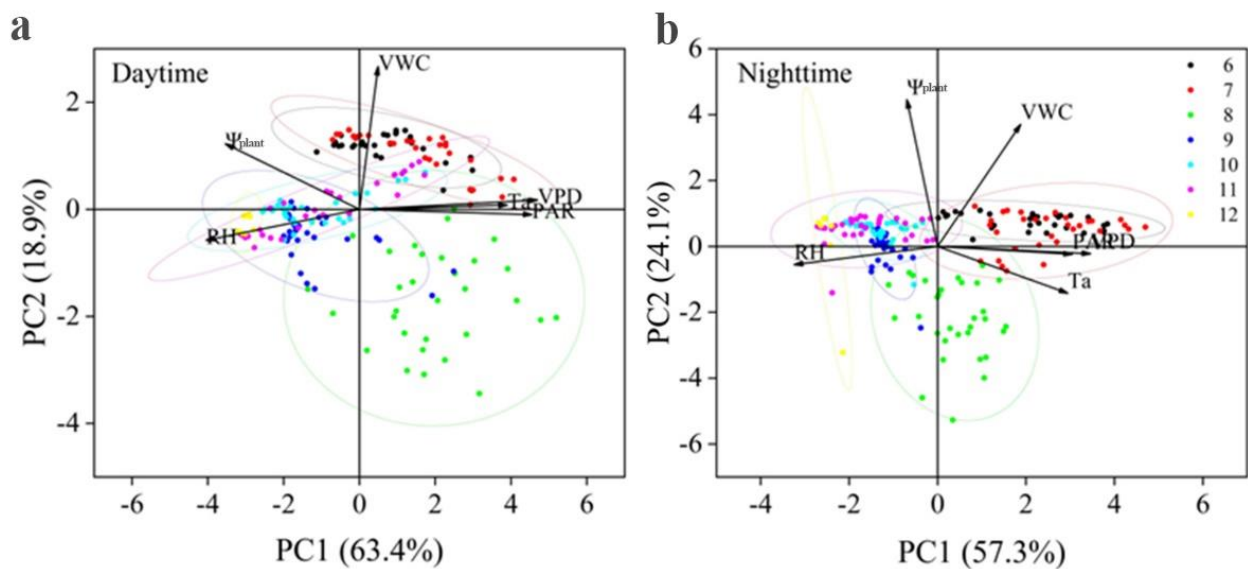


Figure 7. Principal component analysis diagram of environmental factors’ contribution to sap flow. (a) The left side is the response of sap flow to various environmental factors during the day, and (b) the right side is the response of sap flow to various environmental factors at night. Different colored dots represent different months. RH: relative humidity; Ta: air temperature; PAR: photosynthetically active radiation; VPD: vapor pressure deficit; VWC: volumetric water content; Ψ_{plant} : plant water potential.

Table 3. Results of principal component analysis of environmental factors.

Time	Axis Number	Factor Loadings						Total Variance Explained (%)	Cumulative Variance Explained (%)
		RH	Ta	PAR	VPD	VWC	Ψ_{plant}		
period	1	−0.854	0.824	0.898	0.962	0.236	−0.684	61.062	61.062
	2	−0.240	−0.014	−0.162	0.133	0.905	0.570	20.768	81.829

RH: relative humidity; Ta: air temperature; PAR: photosynthetically active radiation; VPD: vapor pressure deficit; VWC: volumetric water content; Ψ_{plant} : plant water potential.

3.4. Variation in Daytime E_{daily} and Night E_{night} of Sap Flow of Golden Pear

The changes in sap flow of pear trees were observed throughout the monitoring period, from growing season to non-growing season; there were significant changes during the day and night (Figure 8). The daytime sap flow in the growing season is about 2.5 times that of the nighttime sap flow. After entering the non-growing season, the daytime sap flow is not much different from the nighttime sap flow. Especially in the non-growing season, it maintained a stable level (Table 4).

The small graph in Figure 8 shows the ratio of day to night pear sap flow over the entire observation period; it can be seen that there is a significant positive correlation between them ($p < 0.05$; $R^2 = 0.741$) and daytime sap flow had a significant positive effect on nighttime flow. Previous analysis of environmental factors showed that VPD is the key factor affecting sap flow; therefore, we conducted a linear regression on the influence of VPD on daytime and nighttime sap flow (Figure 9a,b). The results showed that VPD had a greater impact on the daytime sap flow ($R^2 = 0.6447$); there was a significant positive correlation between them ($p < 0.05$), and the effect of VPD on sap flow at night was relatively limited. We further analyzed the relationship between day and night flow in growing season and non-growing season by linear regression (Figure 9c,d). There was a more positive relationship between day and night flow in the growing season than in the non-growing season. However, the correlation was weaker in non-growing seasons ($R^2 = 0.3101$; $p < 0.05$); it can be clearly seen that the daytime sap flow had a weaker effect than the nighttime.

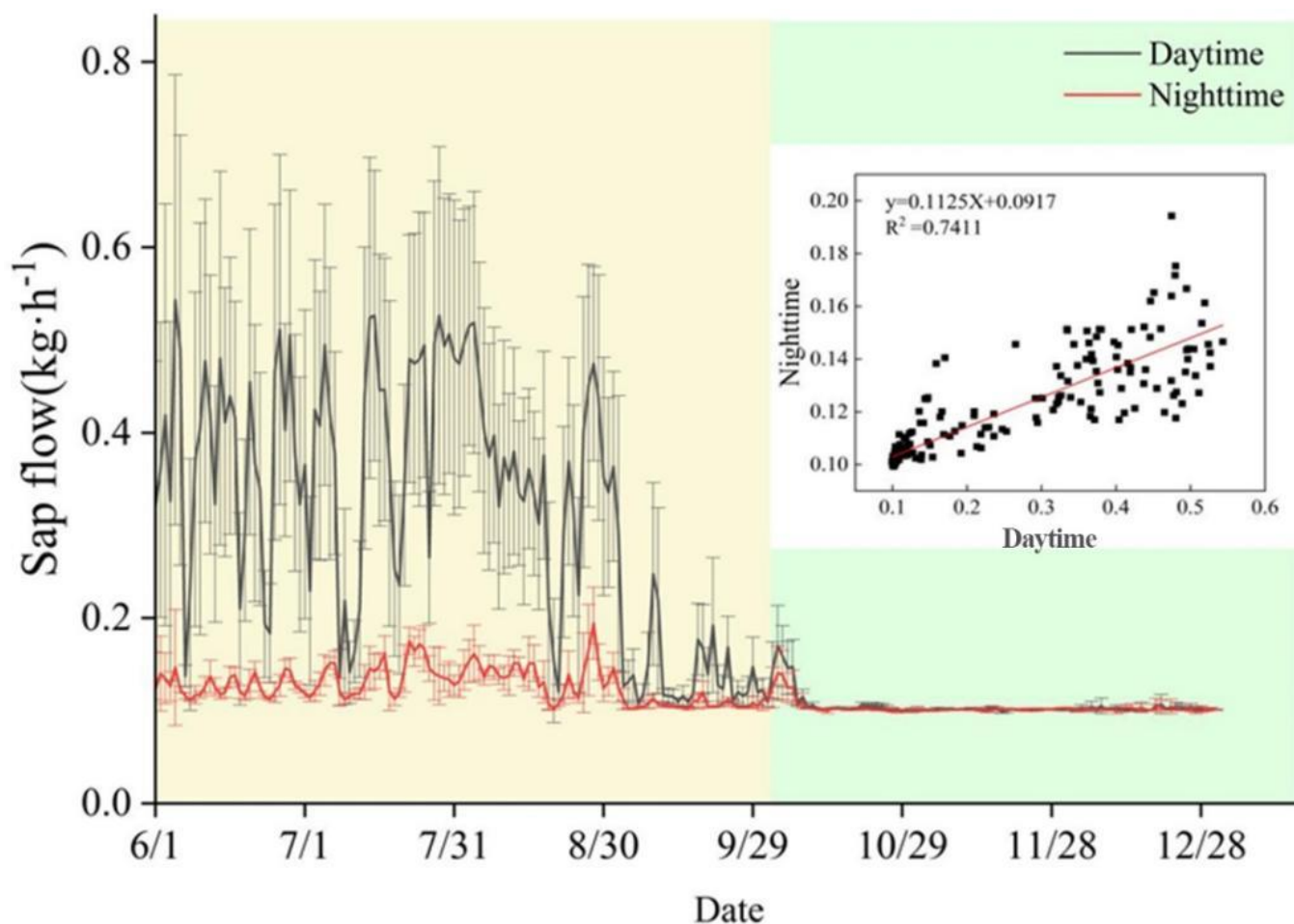


Figure 8. The variation in sap flow of golden pears in the day and night during the whole observation period. In the figure, the light orange areas represent the growing season, and the green areas represent the non-growing season. The black line represents the daytime sap flow value, and the red line represents the nighttime sap flow value. The right panel is a linear regression of daytime and nighttime sap flow over the entire study period. Significance level $p < 0.05$.

Table 4. The difference between the mean sap flow during the day and night of each month.

	June	July	August	September	October	November	December
Daytime	0.373 ^a (0.103)	0.383 ^a (0.124)	0.362 ^a (0.095)	0.151 ^b (0.059)	0.112 ^b (0.019)	0.101 ^b (0.001)	0.102 ^b (0.002)
Nighttime	0.127 ^b (0.010)	0.137 ^a (0.018)	0.139 ^a (0.019)	0.108 ^c (0.009)	0.107 ^c (0.011)	0.101 ^c (0.001)	0.102 ^c (0.001)

The numbers in parentheses represent the standard error of the data, and the lowercase letters in the upper right corner represent the significant difference of a group of data at the $p = 0.05$ level, and combined with the Tukey post-test, multiple comparisons were performed on the continuous measurement data. The same letter indicates that the difference is not significant, and different letters indicate that the difference is significant.

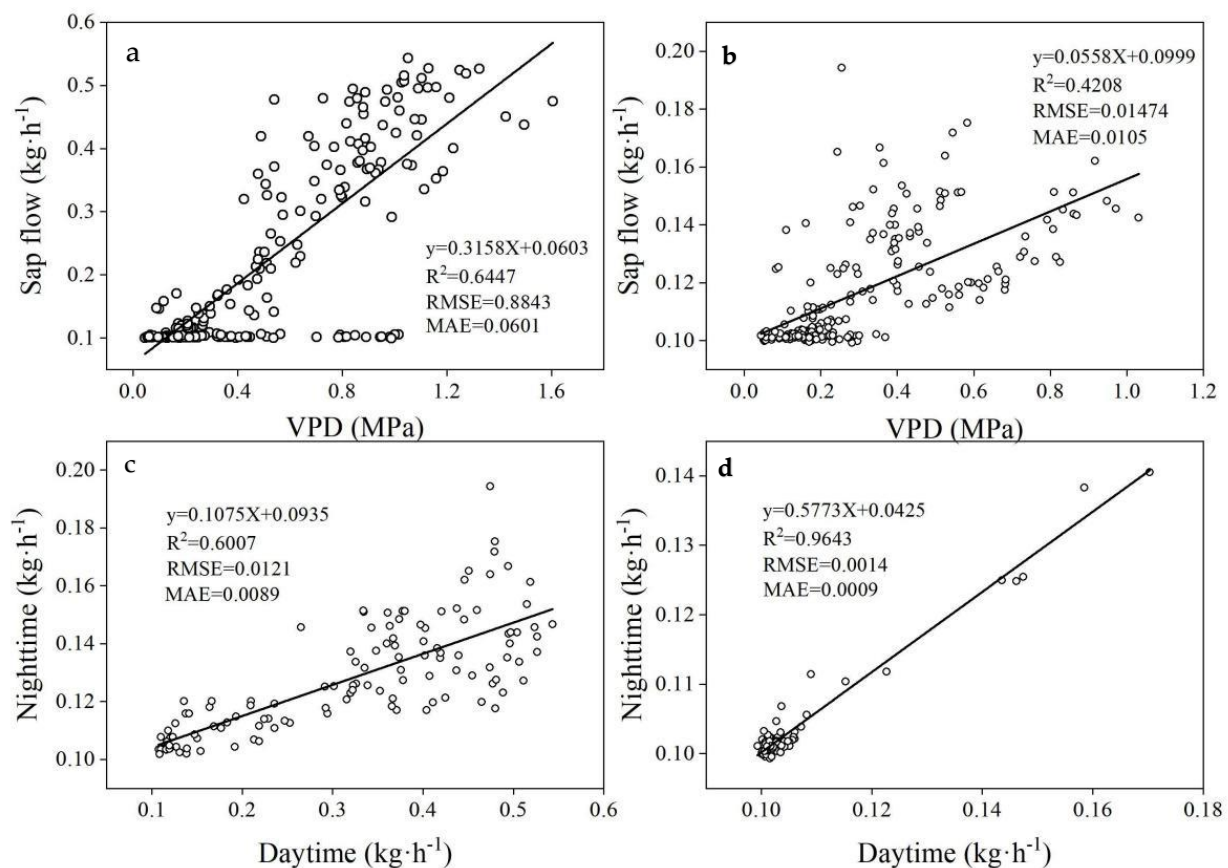


Figure 9. Relationship between VPD and sap flow of golden pear. (a) Linear regression between daytime sap flow and VPD. (b) Linear regression between night sap flow and VPD. (c) and (d) are the relationship between daytime and nighttime sap flow in the growing season and non-growing season, respectively. The significance level was $p < 0.05$. RMSE is root mean square error, MAE is mean absolute value error.

3.5. Differences in Soil Water Potential, Plant Water Potential and Sap Flow

We analyzed soil water content, soil water potential, plant water potential, and sap flow during the observation period (Figure 10), when the significance level was less than 0.05, VWC, Ψ_{soil} , and Ψ_{plant} showed significant differences from month to month. August, in particular, was the lowest. Based on the temperature and precipitation information of the current period, August is the hottest month of the year, with little precipitation (the lowest in the whole growing season (71.2 mm)). Therefore, a soil water content deficit was caused, and the corresponding soil water potential was also at the lowest value (−1324.31 kPa), making it difficult for plants to absorb water. The plant water potential in August also had a very high negative value (−1.21 MPa), indicating that plants were in urgent need of water. Although precipitation was rarer in the non-growing season, soil moisture was higher than in August, and soil water potential and plant water potential were also close to 0 kPa (MPa). Trees need less water, which is probably related to the physiological cycle of the pear itself. August is the period when the fruit of the golden pear expands rapidly. The growth of the fruit increases the tree's demand for water, and, combined with high evaporation and low precipitation, soil water content is consumed greatly and plant water potential is at the lowest level. By the end of September and after October, the golden pear fruits have been picked, the trees have entered a new season of pruning, water needs are limited, evaporation is low, and low rainfall can satisfy its growth.

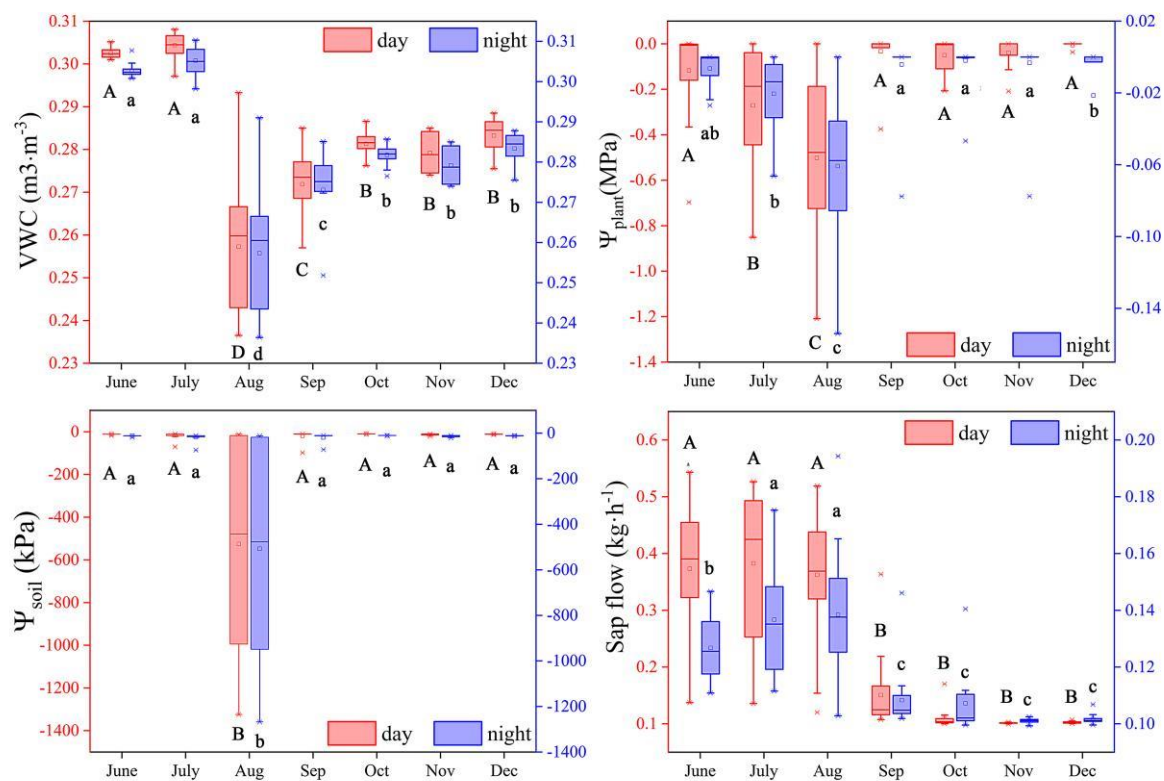


Figure 10. The seasonal changes of VWC, Ψ_{soil} , Ψ_{plant} and sap flow during the whole monitoring period. The red rectangle represents day, and the blue rectangle represents night. Uppercase letters indicate significant differences at the $p = 0.01$ level, and lowercase letters indicate significant differences at the $p = 0.05$ level.

Ψ_{soil} and Ψ_{plant} both reached their lowest values in August. The peak flow occurred in July, and there was no obvious correlation between them. When the soil water potential was less than -388.52 kPa, with the increase in soil water potential, the sap flow generally showed an increasing trend. When the soil water potential was less than -86.56 kPa, the sap flow fluctuated greatly (0.10 – 0.526 $\text{kg}\cdot\text{h}^{-1}$), and may have been affected by environmental factors such as photosynthetically active radiation, saturation vapor pressure difference, and air temperature. Ψ_{plant} was generally negatively correlated with sap flow, in the range of -0.69 to -0.14 MPa, the sap flow decreased. The water potential was close to 0 kPa during most of the non-growing season; at this time, soil water content was basically saturated, plant water demand was limited, and sap flow was low.

4. Discussion

4.1. Sap Flow Characteristics and Influencing Factors during the Observation Period

There are significant differences in sap flow between different tree species and within wood [27]. In this study, we found radial variation of sap flow in all monitored pear tree samples. As Figure 4b shows, the sap flow velocity of the pear trees was the highest at 0.5–1 cm at the xylem edge, reaching 46.21 $\text{cm}\cdot\text{h}^{-1}$, and then it gradually decreased, with the lowest value of 36.03 $\text{cm}\cdot\text{h}^{-1}$ at 2–2.5 cm near the center of the tree. It showed a consistent diurnal variation pattern. The sap flow velocity measured by the two probes inside and outside maintained a small difference at night, and the difference gradually increased during the day, reaching the maximum difference between 12:00 and 15:00. Therefore, in the case of golden pears, the sap flow in the sapwood toward the outside of the tree is much higher than that in the inside of the tree. This is consistent with the findings of Bodo et al. (2021); they installed sensors at different depths in the xylem of temperate Korean pine forests and found that most sap flow occurred in the outermost sapwood (0 – 20 mm > 20 – 40 mm > 40 – 60 mm), within 3 cm of the cambium [28].

In this study, the sap flow of golden pears was significantly different between seasons ($p < 0.05$), which may be due to different water use strategies in different environments [29]. The greatest water stress usually occurs in the summer, due to high temperature and strong evaporation, where soil moisture is low and transpiration is strong, causing trees to lose a lot of water [30]. T_a and PAR reached their maximum value in August, due to the serious lack of precipitation; the VWC was low (23.64–27.91%) and plant sap flow was also the lowest in the growing season in August. This suggests that regardless of the values of other environmental factors such as VPD and T_a , soil moisture may be the most important factor, sap flow is impossible without soil water [31]. Si et al. found, in studying *Populus euphratica* sap flow in desert riparian forest in northwest China, that the soil moisture content was the lowest at days 95–116 (26–29%), and the sap flow was minimal [32]; this is consistent with our findings. In this paper, we found that the relationship between the two was not obvious in the regression analysis of sap flow and soil moisture content; this is inconsistent with Kavanagh et al.'s finding that sap flow was linearly related to soil water content; it is speculated that this may be due to the differences in regions and tree species, and the unique regional environment of the karst area has caused seasonal droughts [33,34]. At this point, the plant may have physiological adjustments that reduce transpiration by closing its stomata; however, long-term drought can also lead to changes in leaf traits or severe water deficit, thus damaging transpiration recovery ability [35,36]. The maximum sap flow of the pear trees was generally synchronous with the peak value of VPD, T_a , and PAR or had a time-lag effect and was positively affected ($p < 0.05$). The delay effect may be due to the slower response of leaf wetness and stomata to photosynthesis [37]. In addition, stomata aperture and stem and leaf morphology also change with light intensity, thus affecting plant photosynthesis and water use efficiency [38,39].

Non-growing season plant sap flow is also an important part of water balance. In our study, it was found that very low sap flow remained after all the leaves were dropped, with almost the same changes in sap flow in November and December (Figure 10). When monitoring deciduous tree species in northern Thailand, Yoshifuji et al. found that the sap flow still changed when the leaf area index was zero. Zhang et al. also found that the sap flow of broad-leaved deciduous trees was lower during the day and night in winter, which is consistent with ours [40,41]. Despite this, there is still a correlation between the flow and VPD, T_a , Ψ_{plant} , and other factors (Figure 7), and the same trend. In particular, our research also found that the peak time of non-growing season flow advanced to around 07:00 or 08:00 (Figure 5), well before midday during the growing season. This means that when soil moisture is limited, transpiration is regulated, and plants start stomata regulation quickly to conserve water, while a later peak time indicates that they are actively transporting water for a longer period of time. This may be related to the fact that the nighttime flow replenishes the previous day's high tree loss, and the variation in soil moisture in winter is low. Lu et al. have shown that the earlier the sap peak occurs, the faster plants can activate stomata regulation to balance water; this behavior is a response to increased VPD and reduced sensitivity of transpiration to soil water changes [42]. They also found that *Quercus liaotungensis* preregulates its stomata to maintain stable transpiration when soil moisture is low; this is similar to our situation. In winter, golden pear has little water demand, and VWC basically meets the plant's survival needs; therefore, the peak value of sap flow is advanced. The different responses of sap flow to soil moisture of tree species in the growing season and in the non-growing season indicated that the species adjusted its water use strategy to adapt to the environment under the change in the external environment [43].

4.2. Physiological and Ecological Significance of Daytime and Nighttime Sap Flow

For the last 20 years, many researchers have found that nocturnal sap flow contributes significantly to tree water balance. In different habitats, the contribution ratio of nocturnal sap flow to total daily sap flow ($E_{\text{night}}/E_{\text{daily}}$) is generally 1–28%. However, in this study, it was 17.3% to 50.7%, the average contribution was 40.1%, and most values were above 40% after the non-growing season (Figure 11). This is far beyond the range of other studies, and

the reason may be related to the growing environment of golden pears, scarce rainfall, and severe drought. E_{night} was simultaneously affected by a variety of environmental factors; Figure 6 shows that it was still affected by VPD, VWC, Ψ_{plant} , etc. E_{night} was positively correlated with VPD at both daily and hourly scales. Under climate change, the increased rate of temperature at night is higher than that of daytime, and high temperature and low humidity will lead to an increase in sap flow at night [44]. In addition, with increased nighttime hydration, E_{night} also increases the tree's predawn water potential, thus reducing the risk of xylem embolism [45,46], which helps in the face of drought stress.

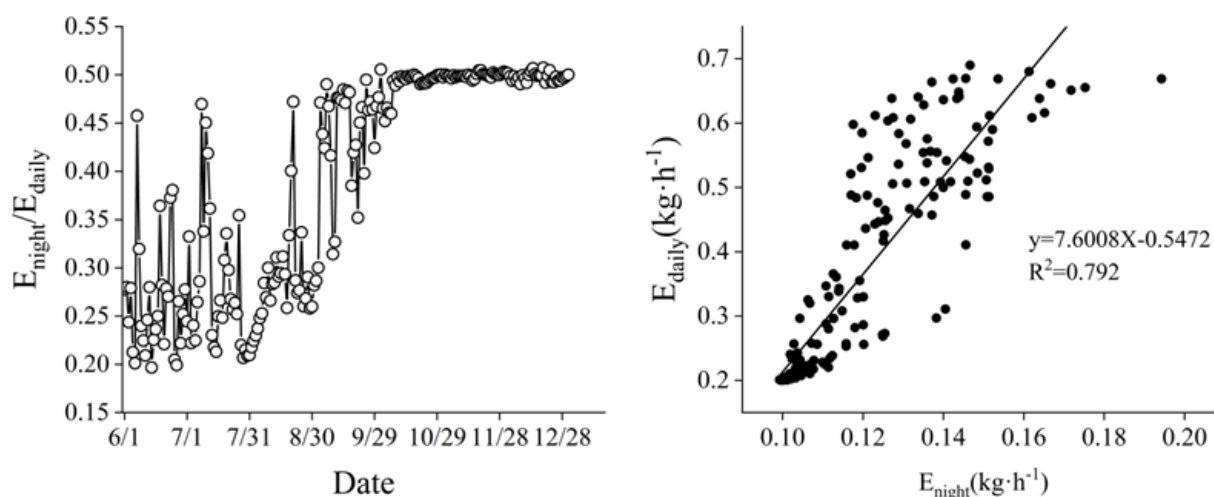


Figure 11. Seasonal variation and linear regression of daytime and nighttime sap flow ratios.

In numerous studies, nocturnal sap flow has been found throughout the life cycle of plants, the more intense the transpiration during the day, the more water is required at night to drive the flow. Dalmolin et al. believed that multiple external factors such as intense evaporation and high temperature weather were the main factors for the occurrence of sap flow in arid areas [47]. However, such a large proportion of nocturnal sap flow is difficult to distinguish as a response to nocturnal transpiration or stem water rehydration, since the two can occur simultaneously and are difficult to separate [48,49]. The correlation between nighttime flow and daytime flow ($R^2 = 0.741$) also shows that nighttime sap flow promotes transpiration the next day, xylem water potential will gradually increase after sunset with the emergence of sap flow, and it reaches its maximum value at around 0:00–02:00 (Figure 5). The results also showed that the seasonal difference in sap flow velocity was not obvious, it slowly decreased from 20:00 to 0:00 and gradually stabilized after midnight. This could mean that the trees' stems have been rehydrated, which will increase the supply of nutrients to the distal part of the canopy and prevent excessive leaf swelling at night [50]. Zhao et al. (2017) showed, in photographs of stomata of *Populus euphratica* in the Alxa Desert, that at least 15% of leaf stomata remain open at night, which will facilitate the flow at night to promote transpiration the next day. Sap flow would promote photosynthesis to start early through rapidly opening stomata [51] and reach the peak of daytime sap flow in advance (Figure 5).

4.3. Research Limitations and Implications

Although this study found a relationship between environmental factors and pear sap flow, there are still obvious shortcomings and limitations. First, the study lasted only seven months and failed to fully monitor the activities of a plant's life cycle, and the data obtained could not fully explain the response of the golden pear stream to environmental factors. Second, since there is radial variability in sap flow velocity, which leads to an overestimation of plant transpiration, the best approach is to measure at different depths in the tree, but this is difficult to achieve due to the cost of money and time [52]. Not only

that, stomatal conductance and tree transpiration are also important factors affecting plant growth. However, due to the limitation of experimental equipment, we lacked data on stomatal conductance and transpiration. Water loss caused by stomatal opening at night not only reduces the water status of plants before dawn, but may also shorten the time during the day when photosynthetic carbon is effectively increased [53]. Especially in hot and arid environments, this effect can reduce the overall water use efficiency of plants; future research needs to strengthen this exploration. In addition, as a species in the karst area, it is strictly restricted by the karst environment. In complex and numerous niches, even adjacent species of the same species differ in species size, climate, time scale and soil properties.

The results of this study have certain reference significance for residents in the karst areas of southern China, and can provide a theoretical basis and practical guidance for precision irrigation in the growing season of golden pears [54]. Throughout the growth of the pear tree, local residents can reduce irrigation during the flowering and budding periods in March and April, forcing the plant's root system to go deeper into the ground. In August and September, when the fruit is inflated, it needs a lot of water to maintain growth. Residents can increase irrigation at this stage to replenish soil moisture in time. Relevant studies have also shown that deficit-adjusted irrigation is not only a water-saving strategy, but a timely and appropriate amount of water stress has a certain positive effect on crop growth, yield and quality [55,56]. Figure 10 also shows that August has the lowest soil water potential for golden pear trees (-1324.31 kPa), which is far beyond the normal limit, making it difficult for plants to absorb water, so some trees will dry up in August every year, or fruit quality will decrease. In case of problems such as low water content and incomplete development, supplementary irrigation during the critical water demand period can avoid water stress and lead to fruit tree yield reduction. Using soil and plant water potential as indicators to control irrigation can ignore the effects of crop soil types, evapotranspiration and rainfall, and can directly characterize the relationship between soil water and plant growth [56]. However, there are certain difficulties in implementation. Under large-scale planting, residents cannot monitor changes in soil and plant water potential, and can only rely on such research results for irrigation guidance.

In future research, we need to further increase the monitoring time, and two or three year sap flow data could better reflect the growth status of plants. Second, to prevent overestimation of transpiration, it is best to install sap flow sensors at different depths of the sample tree. In order to deal with the complexity of karst habitats, we need to expand the research object and scale. How will the same species of trees in different growth environments respond to changes in the external environment? Quantification of plant water potential thresholds can better guide local populations to irrigate in areas with frequent seasonal droughts.

5. Conclusions

Our study found that the sap flow in the golden pear tree showed obvious radial variability, the sap flow in the growing season was much larger than that in the non-growing season, and the sap flow in the daytime was larger than that in the night. During the whole monitoring period, except RH and P, other environmental factors were positively correlated with liquid flow, and VPD was the key factor. In addition, the contribution of nocturnal sap flow to the total sap flow was mostly above 40%, indicating that nocturnal sap flow accounts for a considerable proportion of the tree water budget, and plants in karst areas generally show drought resistance. The results of this study can guide people to better irrigate in the fruit growth period in arid environments, and avoid withering and dying of pear trees, which would have a certain water saving significance.

Supplementary Materials: The following supporting information can be downloaded at: <https://www.mdpi.com/article/10.3390/w14111707/s1>, Figure S1: An overview of the study area and the layout of the instruments. (a) An overview of the study area, (b), (c) and (d) sap flow monitoring instruments; Figure S2: Data map of temperature and precipitation in the study area in 2019 and 2020; Figure S3: Correlations between environmental factors. Sap: sap flow; RH: relative humidity; Ta: air 1temperature; PAR: photosynthetically active radiation; VPD: vapor pressure deficit; VWC: volumetric water content; Ψ_{plant} : plant water potential. Significance level less than 0.05 (two-tailed test).

Author Contributions: B.F. analyzed the data and wrote the manuscript. Z.L. conceptualization, methodology and formal analysis. K.X. review and editing, funding acquisition. Y.L. methodology, modification and supervision. B.F., K.L. and X.Y. Field survey and instrument installation. All members commented on the data analyses and reviewed the manuscript. All authors have read and agreed to the published version of the manuscript.

Funding: This work was supported by the Key Science and Technology Program of Guizhou Province (No. 5411 2017 QianKeHe Pingtai Rencai), Guizhou Science and Technology Project (Guizhou Science and Technology Cooperation Platform Talent [2017]5726-28) and the China Overseas Expertise Introduction Program for Discipline Innovation (D17016).

Institutional Review Board Statement: Not applicable.

Informed Consent Statement: Not applicable.

Data Availability Statement: The data presented in this study are available on request from the corresponding author.

Acknowledgments: We appreciate the anonymous reviewers for their invaluable comments and suggestions on this manuscript.

Conflicts of Interest: The authors declare no conflict of interest.

References

1. Sillmann, J.; Thorarinsdottir, T.; Keenlyside, N.; Schaller, N.; Alexander, L.V.; Hegerl, G.; Seneviratne, S.I.; Vautard, R.; Zhang, X.; Zwiers, F.W. Understanding, modeling and predicting weather and climate extremes: Challenges and opportunities. *Weather Clim. Extrem.* **2017**, *18*, 65–74. [[CrossRef](#)]
2. Zhang, J.-G.; He, Q.-Y.; Shi, W.-Y.; Otsuki, K.; Yamanaka, N.; Du, S. Radial variations in xylem sap flow and their effect on whole-tree water use estimates. *Hydrol. Process.* **2015**, *29*, 4993–5002. [[CrossRef](#)]
3. Yan, M.-J.; Zhang, J.-G.; He, Q.-Y.; Shi, W.-Y.; Otsuki, K.; Yamanaka, N.; Du, S. Sapflow-based stand transpiration in a semiarid natural oak forest on China's loess plateau. *Forests* **2016**, *7*, 227. [[CrossRef](#)]
4. Zhou, H.; Zhao, W.; Zheng, X.; Li, S. Root distribution of *Nitraria sibirica* with seasonally varying water sources in a desert habitat. *J. Plant Res.* **2015**, *128*, 613–622. [[CrossRef](#)]
5. Chang, X.; Zhao, W.; Zhang, Z.; Su, Y. Sap flow and tree conductance of shelter-belt in arid region of China. *Agric. For. Meteorol.* **2006**, *138*, 132–141. [[CrossRef](#)]
6. Shen, Q.; Gao, G.; Fu, B.; Lü, Y. Responses of shelterbelt stand transpiration to drought and groundwater variations in an arid inland river basin of Northwest China. *J. Hydrol.* **2015**, *531*, 738–748. [[CrossRef](#)]
7. Nadal-Sala, D.; Sabaté, S.; Sánchez-Costa, E.; Poblador, S.; Sabater, F.; Gracia, C. Growth and water use performance of four co-occurring riparian tree species in a Mediterranean riparian forest. *For. Ecol. Manag.* **2017**, *396*, 132–142. [[CrossRef](#)]
8. Llorens, P.; Poyatos, R.; Latron, J.; Delgado, J.; Oliveras, I.; Gallart, F. A multi-year study of rainfall and soil water controls on Scots pine transpiration under Mediterranean mountain conditions. *Hydrol. Process.* **2010**, *24*, 3053–3064. [[CrossRef](#)]
9. Guerrieri, R.; Belmecheri, S.; Ollinger, S.V.; Asbjornsen, H.; Jennings, K.; Xiao, J.; Stocker, B.D.; Martin, M.; Hollinger, D.Y.; Bracho-Garrillo, R.; et al. Disentangling the role of photosynthesis and stomatal conductance on rising forest water-use efficiency. *Proc. Natl. Acad. Sci. USA* **2019**, *116*, 16909–16914. [[CrossRef](#)]
10. Hentschel, R.; Hommel, R.; Poschenrieder, W.; Grote, R.; Holst, J.; Biernath, C.; Gessler, A.; Priesack, E. Stomatal conductance and intrinsic water use efficiency in the drought year 2003: A case study of European beech. *Trees* **2015**, *30*, 153–174. [[CrossRef](#)]
11. Zhao, C.Y.; Si, J.H.; Feng, Q.; Yu, T.F.; Du Li, P. Comparative study of daytime and nighttime sap flow of *Populus euphratica*. *Plant Growth Regul.* **2017**, *82*, 353–362. [[CrossRef](#)]
12. Chen, S.; Lin, G.; Huang, J.; Jenerette, G.D. Dependence of carbon sequestration on the differential responses of ecosystem photosynthesis and respiration to rain pulses in a semiarid steppe. *Glob. Chang. Biol.* **2009**, *15*, 2450–2461. [[CrossRef](#)]
13. Pineda-García, F.; Paz, H.; Meinzer, F. Drought resistance in early and late secondary successional species from a tropical dry forest: The interplay between xylem resistance to embolism, sapwood water storage and leaf shedding. *Plant Cell Environ.* **2012**, *36*, 405–418. [[CrossRef](#)]

14. Macinnis-Ng, C.; Wyse, S.; Veale, A.; Schwendenmann, L.; Clearwater, M. Sap flow of the southern conifer, *Agathis australis* during wet and dry summers. *Trees* **2015**, *30*, 19–33. [[CrossRef](#)]
15. Ford, C.R.; Hubbard, R.; Vose, J.M. Quantifying structural and physiological controls on variation in canopy transpiration among planted pine and hardwood species in the southern Appalachians. *Ecohydrology* **2011**, *4*, 183–195. [[CrossRef](#)]
16. Lachenbruch, B.; McCulloh, K.A. Traits, properties, and performance: How woody plants combine hydraulic and mechanical functions in a cell, tissue, or whole plant. *New Phytol.* **2014**, *204*, 747–764. [[CrossRef](#)] [[PubMed](#)]
17. Santini, N.S.; Cleverly, J.; Faux, R.; Lestrangé, C.; Rumman, R.; Eamus, D. Xylem traits and water-use efficiency of woody species co-occurring in the Ti Tree Basin arid zone. *Trees* **2015**, *30*, 295–303. [[CrossRef](#)]
18. Verdaguer, D. Towards a better understanding of the role of rhizomes in mature woody plants: The belowground system of *Quercus coccifera*. *Trees* **2020**, *34*, 903–916. [[CrossRef](#)]
19. Sterck, F.; Markesteijn, L.; Schieving, F.; Poorter, L. Functional traits determine trade-offs and niches in a tropical forest community. *Proc. Natl. Acad. Sci. USA* **2011**, *108*, 20627–20632. [[CrossRef](#)]
20. Burgess, S.S.O.; Adams, M.; Turner, N.C.; Beverly, C.R.; Ong, C.K.; Khan, A.A.H.; Bleby, T.M. An improved heat pulse method to measure low and reverse rates of sap flow in woody plants. *Tree Physiol.* **2001**, *21*, 589–598. [[CrossRef](#)]
21. Forster, M.A. How Reliable Are Heat Pulse Velocity Methods for Estimating Tree Transpiration? *Forests* **2017**, *8*, 350. [[CrossRef](#)]
22. Liu, Z.; Lv, P.; Xu, W. Biological characteristics and key points of cultivation techniques of golden pear. *Fujian Fruit Tree*. **2001**, *3*, 33–35.
23. Xiong, K.N.; LI, J.; Long, M.Z. Features of Soil and Water Loss and Key Issues in Demonstration Areas for Combating Karst Rocky Desertification. *Acta Geogr. Sin.* **2012**, *67*, 878–888. [[CrossRef](#)]
24. Xiong, K.N.; Chi, Y.K. The Problems in Southern China Karst Ecosystem in Southern of China and Its Countermeasures. *Ecol. Econ.* **2015**, *31*, 23–30. [[CrossRef](#)]
25. Granier, A. Evaluation of transpiration in a Douglas-fir stand by means of sap flow measurements. *Tree Physiol.* **1987**, *3*, 309–320. [[CrossRef](#)]
26. Campbell, G.S.; Norman, J.M. *An Introduction to Environmental Biophysics*; Springer Science & Business Media: Berlin/Heidelberg, Germany, 2000.
27. Buyinza, J.; Muthuri, C.W.; Downey, A.; Njoroge, J.; Denton, M.D.; Nuberg, I.K. Contrasting water use patterns of two important agroforestry tree species in the Mt Elgon region of Uganda. *Aust. For.* **2019**, *82*, 57–65. [[CrossRef](#)]
28. Bodo, A.V.; Arain, M.A. Radial variations in xylem sap flux in a temperate red pine plantation forest. *Ecol. Process.* **2021**, *10*, 24. [[CrossRef](#)]
29. Grossiord, C.; Gessler, A.; Granier, A.; Pollastrini, M.; Bussotti, F.; Bonal, D. Interspecific competition influences the response of oak transpiration to increasing drought stress in a mixed Mediterranean forest. *For. Ecol. Manag.* **2014**, *318*, 54–61. [[CrossRef](#)]
30. Alvarado-Barrientos, M.; Holwerda, F.; Asbjornsen, H.; Dawson, T.; Bruijnzeel, L. Suppression of transpiration due to cloud immersion in a seasonally dry Mexican weeping pine plantation. *Agric. For. Meteorol.* **2014**, *186*, 12–25. [[CrossRef](#)]
31. Huang, C.; Domec, J.-C.; Ward, E.J.; Duman, T.; Manoli, G.; Parolari, A.J.; Katul, G. The effect of plant water storage on water fluxes within the coupled soil-plant system. *New Phytol.* **2016**, *213*, 1093–1106. [[CrossRef](#)]
32. Si, J.; Feng, Q.; Yu, T.; Zhao, C. Nighttime sap flow and its driving forces for *Populus euphratica* in a desert riparian forest, Northwest China. *J. Arid Land.* **2015**, *7*, 665–674. [[CrossRef](#)]
33. Yan, C.; Wang, B.; Zhang, Y.; Zhang, X.; Takeuchi, S.; Qiu, G.Y. Responses of Sap Flow of Deciduous and Conifer Trees to Soil Drying in a Subalpine Forest. *Forests* **2018**, *9*, 32. [[CrossRef](#)]
34. Kavanagh, K.L.; Pangle, R.; Schotzko, A.D. Nocturnal transpiration causing disequilibrium between soil and stem predawn water potential in mixed conifer forests of Idaho. *Tree Physiol.* **2007**, *27*, 621–629. [[CrossRef](#)] [[PubMed](#)]
35. Wang, L.; Dai, Y.; Sun, J.; Wan, X. Differential hydric deficit responses of *Robinia pseudoacacia* and *Platycladus orientalis* in pure and mixed stands in northern China and the species interactions under drought. *Trees* **2017**, *31*, 2011–2021. [[CrossRef](#)]
36. Jiao, L.; Lu, N.; Sun, G.; Ward, E.J.; Fu, B. Biophysical controls on canopy transpiration in a black locust (*Robinia pseudoacacia*) plantation on the semi-arid Loess Plateau, China. *Ecohydrology* **2015**, *9*, 1068–1081. [[CrossRef](#)]
37. Fang, W.; Lu, N.; Zhang, Y.; Jiao, L.; Fu, B. Responses of nighttime sap flow to atmospheric and soil dryness and its potential roles for shrubs on the Loess Plateau of China. *J. Plant Ecol.* **2017**, *11*, 717–729. [[CrossRef](#)]
38. Ghorbanzadeh, P.; Aliniaieifard, S.; Esmaeili, M.; Mashal, M.; Azadegan, B.; Seif, M. Dependency of Growth, Water Use Efficiency, Chlorophyll Fluorescence, and Stomatal Characteristics of Lettuce Plants to Light Intensity. *J. Plant Growth Regul.* **2020**, *40*, 2191–2207. [[CrossRef](#)]
39. Bloemen, J.; Vergeynst, L.L.; Overlaet-Michiels, L.; Steppe, K. How important is woody tissue photosynthesis in poplar during drought stress? *Trees* **2014**, *30*, 63–72. [[CrossRef](#)]
40. Yoshifuji, N.; Komatsu, H.; Kumagai, T.; Tanaka, N.; Tantasirin, C.; Suzuki, M. Interannual variation in transpiration onset and its predictive indicator for a tropical deciduous forest in northern Thailand based on 8-year sap-flow records. *Ecohydrology* **2011**, *4*, 225–235. [[CrossRef](#)]
41. Zhang, Z.Z.; Zhao, P.; McCarthy, H.R.; Zhao, X.H.; Niu, J.F.; Zhu, L.W.; Ni, G.Y.; Ouyang, L.; Huang, Y.Q. Influence of the decoupling degree on the estimation of canopy stomatal conductance for two broadleaf tree species. *Agric. For. Meteorol.* **2016**, *221*, 230–241. [[CrossRef](#)]

42. Lyu, J.; He, Q.-Y.; Yang, J.; Chen, Q.-W.; Cheng, R.-R.; Yan, M.-J.; Yamanaka, N.; Du, S. Sap flow characteristics in growing and non-growing seasons in three tree species in the semiarid Loess Plateau region of China. *Trees* **2020**, *34*, 943–955. [[CrossRef](#)]
43. Forster, M.A. How significant is nocturnal sap flow? *Tree Physiol.* **2014**, *34*, 757–765. [[CrossRef](#)] [[PubMed](#)]
44. Attia, Z.; Domec, J.-C.; Oren, R.; Way, D.A.; Moshelion, M. Growth and physiological responses of isohydric and anisohydric poplars to drought. *J. Exp. Bot.* **2015**, *66*, 4373–4381. [[CrossRef](#)] [[PubMed](#)]
45. Cirelli, D.; Equiza, M.A.; Lieffers, V.J.; Tyree, M.T. *Populus* species from diverse habitats maintain high night-time conductance under drought. *Tree Physiol.* **2016**, *36*, 229–242. [[CrossRef](#)]
46. Ogle, K.; Lucas, R.W.; Bentley, L.P.; Cable, J.M.; Barron-Gafford, G.A.; Griffith, A.; Ignace, D.; Jenerette, G.D.; Tyler, A.; Huxman, T.E.; et al. Differential daytime and night-time stomatal behavior in plants from North American deserts. *New Phytol.* **2012**, *194*, 464–476. [[CrossRef](#)]
47. Dalmolin, Â.C.; Lobo, F.A.; Vourlitis, G.; Silva, P.R.; Dalmagro, P.R.; Antunes, M.Z., Jr.; Ortíz, C.E.R. Is the dry season an important driver of phenology and growth for two Brazilian savanna tree species with contrasting leaf habits? *Plant Ecol.* **2014**, *216*, 407–417. [[CrossRef](#)]
48. Daley, M.J.; Phillips, N.G. Interspecific variation in nighttime transpiration and stomatal conductance in a mixed New England deciduous forest. *Tree Physiol.* **2006**, *26*, 411–419. [[CrossRef](#)]
49. Ma, C.; Luo, Y.; Shao, M.; Li, X.; Sun, L.; Jia, X. Environmental controls on sap flow in black locust forest in Loess Plateau, China. *Sci. Rep.* **2017**, *7*, 13160. [[CrossRef](#)]
50. Donovan, L.; Linton, M.J.; Richards, J.H. Predawn plant water potential does not necessarily equilibrate with soil water potential under well-watered conditions. *Oecologia* **2001**, *129*, 328–335. [[CrossRef](#)]
51. Yu, T.; Feng, Q.; Si, J.; Zhang, X.; Alec, D.; Zhao, C. Evidences and magnitude of nighttime transpiration derived from *Populus euphratica* in the extreme arid region of China. *J. Plant Biol.* **2016**, *59*, 648–657. [[CrossRef](#)]
52. Čermák, J.; Cienciala, E.; Kučera, J.; Hällgren, J.-E. Radial velocity profiles of water flow in trunks of Norway spruce and oak and the response of spruce to severing. *Tree Physiol.* **1992**, *10*, 367–380. [[CrossRef](#)]
53. Delzon, S.; Sartore, M.; Granier, A.; Loustau, D. Radial profiles of sap flow with increasing tree size in maritime pine. *Tree Physiol.* **2004**, *24*, 1285–1293. [[CrossRef](#)] [[PubMed](#)]
54. Matheny, A.M.; Bohrer, G.; Vogel, C.S.; Morin, T.H.; He, L.; Frasson, R.P.D.M.; Mirfenderesgi, G.; Schäfer, K.V.R.; Gough, C.M.; Ivanov, V.Y.; et al. Species-specific transpiration responses to intermediate disturbance in a northern hardwood forest. *J. Geophys. Res. Biogeosci.* **2014**, *119*, 2292–2311. [[CrossRef](#)]
55. Skubel, R.; Arain, M.A.; Peichl, M.; Brodeur, J.; Khomik, M.; Thorne, R.; Trant, J.; Kula, M. Age effects on the water-use efficiency and water-use dynamics of temperate pine plantation forests. *Hydrol. Process.* **2015**, *29*, 4100–4113. [[CrossRef](#)]
56. Consoli, S.; Stagno, F.; Rocuzzo, G. Sustainable management of limited water resources in a young orange orchard. *Agric. Water Manag.* **2014**, *132*, 60–68. [[CrossRef](#)]